Magnetic quantum phase transitions in Kondo lattices

TOPICAL REVIEW

Magnetic quantum phase transitions in Kondo lattices

Qimiao Si[1], Jian-Xin Zhu[2] and D R Grempel[3]

[1] Department of Physics and Astronomy, Rice University, Houston, TX 77005-1892, USA
[2] Theoretical Division, Los Alamos National Laboratory, Los Alamos, NM 87545, USA
[3] CEA-Saclay, DSM/DRECAM/SPCSI, 91191 Gif-sur-Yvette, France

Abstract
The identification of magnetic quantum critical points in heavy fermion metals
has provided an ideal setting for experimentally studying quantum criticality.
Motivated by these experiments, considerable theoretical efforts have recently
been devoted to re-examining the interplay between Kondo screening and
magnetic interactions in Kondo lattice systems. A local quantum critical
picture has emerged, in which magnetic interactions suppress Kondo screening
precisely at the magnetic quantum critical point (QCP). The Fermi surface
undergoes a large reconstruction across the QCP and the coherence scale
of the Kondo lattice vanishes at the QCP. The dynamical spin susceptibility
exhibits ω/T scaling and non-trivial exponents describe the temperature and
frequency dependences of various physical quantities. These properties are
to be contrasted with the conventional spin density wave picture, in which
the Kondo screening is not suppressed at the QCP and the Fermi surface
evolves smoothly across the phase transition. In this article we discuss recent
microscopic studies of Kondo lattices within an extended dynamical mean
field theory (EDMFT). We summarize the earlier work based on an analytical
ϵ-expansion renormalization group method, and expand on the more recent
numerical results. We also discuss the issues that have been raised concerning
the magnetic phase diagram. We show that the zero-temperature magnetic
transition is second order when double counting of the Ruderman–Kittel–
Kasuya–Yosida interactions is avoided in EDMFT.

(Some figures in this article are in colour only in the electronic version)

Contents

1. Introduction

Heavy fermions started out as a fertile ground on which to study strongly correlated Fermi liquids and superconductors [1]. There was a great deal of amazement at seeing a Fermi liquid whose quasiparticle mass is over a hundred times the bare electron mass; hence the name of the field. It was also surprising to find superconductors in an inherently magnetic environment: the existence of local magnetic moments in these materials is established through the observation of a Curie–Weiss susceptibility at intermediate temperatures (of the order of 100 K), and magnetism is supposed to be 'hostile' to superconductivity. It was qualitatively understood that the large mass reflects the Kondo screening of the magnetic moments, which is necessary to overcome magnetism [2, 3], and the proper theoretical description of the Fermi liquid state [4] was subsequently achieved. When high temperature superconductors were discovered in 1986, the development of the heavy fermion field was naturally interrupted—at least partially. The hiatus proved to be relatively short-lived. As it re-emerged, however, the field acquired a considerably different outlook, with the emphasis now placed on non-Fermi liquid behaviour and magnetic quantum phase transitions. Since the late 1990s the field has become a focal point [5] for the general study of quantum criticality. The interest in QCPs is by no means unique to heavy fermions; it also arises in high temperature superconductors among other materials [3, 6]. However, heavy fermions are particularly advantageous in one important regard. That is, second-order quantum phase transitions are explicitly observed in a growing list of materials of this family.

The QCP in heavy fermions typically separates an antiferromagnetic metallic phase from a paramagnetic metallic phase. Near the magnetic QCP, transport and thermodynamical properties develop anomalies. The $T = 0$ spin density wave (SDW) picture [7–10] describes the QCP in terms of fluctuations of the magnetic order parameter—the paramagnons—both in space and in time. This theory amounts to a ϕ^4 theory—with ϕ being the paramagnon field—with an effective dimensionality of $d_{\text{eff}} = d + z$. Here, z is the dynamic exponent, and is equal to 2 in the antiferromagnetic case. So, d_{eff} is above the upper critical dimension, 4, of the ϕ^4 theory, for spatial dimensions $d \geqslant 2$. The corresponding fixed point is Gaussian. In this picture, the non-Fermi liquid properties of the QCP reflect the singular scattering of electrons by the paramagnons and are unrelated to the process of Kondo screening.

The most direct indication of the unusual nature of the heavy fermion quantum criticality came from inelastic neutron scattering experiments [11, 13]. The magnetic dynamics shows a fractional exponent and ω/T scaling over an extended range of momentum space. These features deviate drastically from the expectations of the SDW theory. Since the SDW critical

fixed point is Gaussian, spin damping would be controlled by some (dangerously) irrelevant coupling, and neither fractional exponent nor ω/T scaling would be expected.

One way to resolve this impasse invokes the breakdown of Kondo screening at the magnetic quantum critical point. On the paramagnetic side, local moments become entangled with the conduction electrons and, in the process, are delocalized and a part of the electron fluid. At the magnetic QCP, the magnetic fluctuations turn soft and act as a source of dissipation that couples to the local moments; this coupling competes with the Kondo interactions and destroys the Kondo screening. Going from the paramagnetic side to the QCP, the electronic excitations depart from those of a Fermi liquid and acquire a non-Fermi liquid form. These non-Fermi liquid excitations are part of the quantum critical spectrum. Unlike the paramagnons, they are characterized by an interacting fixed point. As the control parameter is tuned further, into the magnetically ordered side, the system is again a Fermi liquid, but the Kondo effect is completely destroyed. An important corollary of this picture [15] is that the Fermi surface has a sharp jump at the QCP.

To microscopically study the magnetic quantum phase transition requires an approach that can handle not only the heavy fermion and magnetic states but also the dynamical competition between the two on an equal footing. One suitable approach (if not the only one so far) is extended dynamical mean field theory (EDMFT) [16–19].

In this article, we discuss the EDMFT studies of the Kondo lattice system. In addition to giving a brief summary of the earlier analytical works [15], we will pay particular attention to two issues. The first one deals with the magnetic dynamics near the QCP. A fractional dynamical spin susceptibility exponent accompanies the destruction of Kondo screening [20]. The second one concerns the nature of the zero-temperature transition. When the EDMFT is implemented such that there is no double counting of the static component of the Ruderman–Kittel–Kasuya–Yosida (RKKY) interactions, the transition turns out to be second order [21]. We compare these results with those from some recent related works [22–24].

2. The model, the phases and the phase transitions

2.1. Kondo lattice model

We consider a Kondo lattice model,

$$\mathcal{H} = \mathcal{H}_f + \mathcal{H}_c + \mathcal{H}_K. \tag{1}$$

Here, the f electron component

$$\mathcal{H}_f = \tfrac{1}{2} \sum_{ij} I_{ij}^a S_i^a S_j^a, \tag{2}$$

describes the interactions between spin-$\frac{1}{2}$ local moments and $a = x, y, z$ are the spin projections. We have taken the valence fluctuations to be completely frozen, which should give a good description of at least those heavy fermion metals that have a heavy effective mass and that are undergoing a magnetic quantum phase transition. Without loss of generality, we have assumed that a unit cell contains one local moment (S_i), whose spin-$\frac{1}{2}$ nature reflects the projection onto the lowest Kramers doublet. I_{ij}^a describes the RKKY exchange interaction between the local moments. In the physical systems, the RKKY interaction is generated by the Kondo interactions. Here, we have taken it as an independent parameter, for two reasons. First, it is useful to do so for the purpose of specifying the global phase diagram. Second, as will be seen below, in the EDMFT approach to the Kondo lattice, it is necessary to include this parameter at the Hamiltonian level to treat its effects dynamically (see sections 3 and 4 for details).

The conduction electron component of equation (1) is simply

$$\mathcal{H}_c = \sum_{\mathbf{k}\sigma} \epsilon_{\mathbf{k}} c^\dagger_{\mathbf{k}\sigma} c_{\mathbf{k}\sigma}. \tag{3}$$

It is implicitly assumed that the conduction electrons alone would form a Fermi liquid, and the residual interaction (Landau) parameters for the conduction electron component alone can be neglected. We will consider the number of conduction electrons per unit cell, x, to be in the range $0 < x < 1$; in addition, we will assume that it is not too small, so that the physical RKKY interaction between the nearest-neighbouring local moments is antiferromagnetic, and not too close to 1, so that the Kondo insulating physics does not come into play. All the phases described below are metallic.

Finally, the local moments interact with $\mathbf{s}_{c,i}$, the spins of the conduction electrons, through an antiferromagnetic Kondo coupling J_K:

$$\mathcal{H}_K = \sum_i J_K \mathbf{S}_i \cdot \mathbf{s}_{c,i}. \tag{4}$$

2.2. Kondo effect and magnetic quantum phase transition

For qualitative considerations, consider the Kondo lattice model with a fixed value of I and W, with a small ratio I/W; here I is the typical (say, nearest-neighbour) interaction of H_f, and W the conduction electron bandwidth. We further assume that H_f has an Ising anisotropy. In the antiferromagnetic phase of H_f, the spin excitation spectrum is fully gapped. An infinitesimal J_K cannot lead to any Kondo screening. Hence, the Fermi surface encloses only the conduction electrons, whose number is x per paramagnetic unit cell. We label this phase AF_S.

On the other hand, when J_K dominates over I, the standard Kondo screening does occur. Each local moment is converted into a spin-$\frac{1}{2}$ charge e Kondo resonance. The Fermi surface now encloses not only the conduction electrons but also the local moments, the total number being $1 + x$ per unit cell. We label this phase PM_L. While the existence of this phase is well established [4], the easiest physical way to see it is to consider the limit $J_K \gg W \gg I$. (Since the Kondo state restores $SU(2)$ symmetry, we have, without loss of generality, taken the Kondo exchange coupling to be spin isotropic in equation (4).) In this limit, there is a large binding energy (of the order of $-J_K$) for a local singlet between $\mathbf{S}_i$ and $\mathbf{s}_{c,i}$, and we can safely project to this singlet subspace. In this subspace, $x = 1$ becomes special: here each local moment is locally paired up with a conduction electron, and the entire system becomes a Kondo insulator. For a system of a total of $\mathcal{N}$ unit cells, $x < 1$ amounts to creating $(1 - x)\mathcal{N}$ unpaired local moments, each of which is equivalent to creating a hole in the singlet background. The Kondo lattice model becomes equivalent to an effective single-band Hubbard model of $(1 - x)$ holes per site, with an infinite on-site repulsion (it is impossible to create two holes—there is only one electron in the singlet to begin with) [25, 26]. In the paramagnetic phase, the Luttinger theorem then ensures that the Fermi volume contains $(1 - x)$ holes or, equivalently, $(1 + x)$ electrons!

These general arguments show that the AF_S and PM_L phases are two stable metallic phases. They differ in two important respects. The AF_S is magnetically ordered while the PM_L is not. Equally important, the PM_L has the Kondo screening while the AF_S does not. Increasing the ratio $\delta \equiv J_K/I$ takes the system from AF_S to PM_L. A key question is this: Does the destruction of magnetism and the onset of Kondo screening occur at the same stage? If so, the transition is distinctly different from the $T = 0$ SDW picture. If not—i.e., if the destruction of magnetism happens after the Kondo screening has already set in—then the magnetic transition can be interpreted as an SDW instability of the quasiparticles near the large Fermi surface; the transition goes back to the realm of the $T = 0$ SDW transition picture.

Microscopical studies provide a way to address this issue. A suitable method has to capture not only the AF_S and PM_L phases, due respectively to the RKKY exchange interactions and the Kondo interactions, but also the dynamical competition between these interactions; this dynamical interplay is crucial for the transition region. At this stage, the EDMFT method is the only one we are aware of which fits this requirement.

Of course, microscopic studies always have limitations. Approximations are inevitably used, in the process of solving a Hamiltonian or at the level of the model itself (or both). Controlled approximations, nonetheless, provide us with not only ways of understanding experiments but also intuitions that serve as a basis for more macroscopic approaches. This general philosophy is readily reflected in the EDMFT approach. Even though it is 'conserving' (i.e., satisfying thermodynamic consistency requirements), it assumes that the dependences on $\mathbf{q}$ of some irreducible single-electron and collective quantities ($M(\omega)$ and $\Sigma(\omega)$ defined in the next section) are unimportant.

There are several reasons to believe that the EDMFT approach is useful for the antiferromagnetic quantum transitions at hand. First, because staggered magnetization is not a conserved quantity, the spin damping does not have to acquire a strong dependence on $\mathbf{q}$. This is especially true for metallic systems, where the dynamic exponent z associated with the long-wavelength magnetic fluctuations is larger than 1. In the SDW case [7], for instance, $z = 2$ and $M(\mathbf{q}, \omega)$ can simply be taken as a linear function of $|\omega|$ without any singular dependence on $\mathbf{q}$. Whether the dependence on $\mathbf{q}$ of $M(\mathbf{q}, \omega)$ is singular or normal can be stated in terms of the anomalous spatial dimension η characterizing the long-wavelength fluctuations in space: a non-zero η means that the $\mathbf{q}$ dependence of $M(\mathbf{q}, \omega)$ is more singular than that $[(\mathbf{q} - \mathbf{Q})^2]$ already incorporated in $I_{\mathbf{q}}$. So, if $\eta \neq 0$, the EDMFT is expected to fail, at least for the asymptotic behaviour. For instance, the classical critical points associated with a finite temperature magnetic transition for $d = 2, 3$ must have a finite η; the EDMFT turns out to produce (an artificial) first-order phase transition. For a quantum critical point, on the other hand, long-wavelength fluctuations occur for $d_{\text{eff}} = d + z$ dimensions. There is then a greater likelihood for the vanishing of the spatial anomalous dimension, in which case the $\mathbf{q}$ dependence of $M(\mathbf{q}, \omega)$ is not singular and neglecting it will not change the universal behaviour.

Second, as we have already discussed, the different classes of magnetic quantum critical points of a Kondo lattice can be classified in terms of whether the Fermi surface (in the paramagnetic zone), which is large in the paramagnetic metallic phase, stays large as the QCP is crossed or becomes small by ejecting the local moments. Such large versus small Fermi surfaces are well described in terms of whether the Kondo effect is preserved or destroyed, which, in turn, is readily captured by the EDMFT approach.

We now turn to the EDMFT studies of the Kondo lattice model.

3. Destruction of the Kondo effect within EDMFT

3.1. The EDMFT equations for the paramagnetic phase

The EDMFT approach treats certain intersite (coherent and incoherent) collective effects on an equal footing with the local interaction effects. The EDMFT equations have been constructed in terms of a 'cavity' method [16], diagrammatics [17] and a functional formalism [18]. All of these constructions yield the same dynamical equations. In the diagrammatic language, the EDMFT is seen as entirely different from a systematic expansion [27, 28] in $1/d$ whose zeroth order would correspond to the dynamical mean field theory (DMFT) [28, 29]. Instead, the EDMFT is a resummation scheme that incorporates an infinite series of processes associated

with the intersite collective effects, in addition to the local processes already taken into account in the DMFT. Unlike the single-electron properties, the collective modes do not have a chemical potential. In other words, the bottom of a 'band' is important and this provides a means for spatial dimensionality to come into play in the EDMFT.

Within the EDMFT, the collective effects are organized in terms of an explicit intersite interaction term at the Hamiltonian level. For the Kondo lattice model described in the previous section, this is the intersite exchange term, $\mathcal{H}_f$ of equation (2).

There are several ways to see the details of this formalism. One way is to focus on a spin cumulant [17], whose inverse, $M(\omega)$, is colloquially referred to as a spin self-energy matrix. While it can be rigorously defined for any spinful many-body problem, this quantity is taken as $\mathbf{q}$ independent in the EDMFT.

The dynamical spin susceptibility, on the other hand, is $\mathbf{q}$ dependent and is given by

$$\chi^a(\mathbf{q}, \omega) = \frac{1}{M^a(\omega) + I_\mathbf{q}^a}. \tag{5}$$

The conduction electron self-energy is still given by $\Sigma(\omega)$, and the conduction electron Green's function retains the standard form:

$$G(\mathbf{k}, \epsilon) = \frac{1}{\epsilon + \mu - \epsilon_\mathbf{k} - \Sigma(\epsilon)}. \tag{6}$$

The irreducible quantities, $M(\omega)$ and $\Sigma(\epsilon)$, are determined in terms of a self-consistent Bose–Fermi Kondo model:

$$\mathcal{H}_{\mathrm{imp}} = J_K \mathbf{S} \cdot \mathbf{s}_c + \sum_{p,\sigma} E_p c_{p\sigma}^\dagger c_{p\sigma} + g \sum_{p,a} S^a(\phi_{p,a} + \phi_{-p,a}^\dagger) + \sum_{p,a} w_{p,a} \phi_{p,a}^\dagger \phi_{p,a}. \tag{7}$$

The self-consistency reflects the translational invariance:

$$\begin{aligned} \chi_{\mathrm{loc}}^a(\omega) &= \sum_\mathbf{q} \chi^a(\mathbf{q}, \omega), \\ G_{\mathrm{loc}}(\omega) &= \sum_\mathbf{k} G(\mathbf{k}, \omega). \end{aligned} \tag{8}$$

When combined with the Dyson equations, $M^a(\omega) = \chi_{0,a}^{-1}(\omega) + 1/\chi_{\mathrm{loc}}^a(\omega)$ and $\Sigma(\omega) = G_0^{-1}(\omega) - 1/G_{\mathrm{loc}}(\omega)$, where $\chi_{0,a}^{-1}(\omega) = -g^2 \sum_p 2w_{p,a}/[\omega^2 - w_{p,a}^2]$ and $G_0(\omega) = \sum_p 1/(\omega - E_p)$ are the Weiss fields, these self-consistency equations specify the dispersions, E_p and $w_{p,a}$, and the coupling constant g.

We will focus on the case of two-dimensional magnetic fluctuations, characterized by the RKKY density of states $\rho_I(\epsilon) \equiv \sum_\mathbf{q} \delta(\epsilon - I_\mathbf{q}) = (1/2I)\Theta(I - |\epsilon|)$. The first of equations (8) becomes

$$\begin{aligned} M^a(\omega) &= I/\tanh[I\chi_{\mathrm{loc}}^a(\omega)] \\ &= I + 2I \exp\left[-2I\chi_{\mathrm{loc}}^a(\omega)\right] + \cdots \end{aligned} \tag{9}$$

where the last equality is an expansion in terms of $\exp[-2I\chi_{\mathrm{loc}}^a(\omega)]$, valid when the local susceptibility is divergent.

3.2. Destruction of the Kondo effect

Both the Kondo screening and its destruction are encoded in the Bose–Fermi Kondo model, equation (7). The antiferromagnetic Kondo coupling (J_K) is responsible for the formation of a Kondo singlet in the ground state and the concomitant generation of a Kondo resonance in the excitation spectrum. The coupling of the local moment to the dissipative bosonic bath (g)

provides a competing mechanism. To see this in some detail, we first analyse equation (7) alone without worrying about the self-consistency conditions. We consider a given spectrum of the bosonic bath,

$$\sum_p [\delta(\omega - w_{p,a}) - \delta(\omega + w_{p,a})] \propto |\omega|^{1-\epsilon} \, \mathrm{sgn} \, \omega. \tag{10}$$

The problem can be studied using an ϵ-expansion [30]. For small g, the Kondo coupling dominates, leading to a Kondo screening. A sufficiently large coupling g destroys the Kondo screening completely, reaching a local moment phase. The transition between these two phases is of second order, and is described by a QCP where the Kondo screening is just destroyed and the electronic excitations have a non-Fermi liquid form. The local spin susceptibility has a Pauli form on the Kondo side. The destruction of Kondo screening is then manifested in a divergent local susceptibility at the QCP. An important property that is shared by the Bose–Fermi Kondo model with $SU(2)$ spin symmetry, XY spin anisotropy or Ising spin anisotropy is that $\chi_{\mathrm{loc}}^a(\tau) \sim 1/\tau^\epsilon$, at the QCP. Here, $a = x, y, z$, $a = x, y$ and $a = z$ for the $SU(2)$, XY and Ising cases, respectively.

Correspondingly,

$$\chi_{\mathrm{loc}}^a(\omega) = A^a(\epsilon)/(-\mathrm{i}\omega)^{1-\epsilon}. \tag{11}$$

While the critical amplitude, $A^a(\epsilon)$, depends on the spin anisotropy, the critical exponent does not; it is equal to $1 - \epsilon$ in all cases.

There is an important point that follows from the above analysis which we will use in the following discussion of the numerical results. Within the EDMFT approach to the Kondo lattice, if the local spin susceptibility of the Kondo lattice model is divergent at the magnetic QCP, the corresponding local problem is sitting on the critical manifold. In other words, a divergent local susceptibility is a signature of the critical Kondo screening and its associated non-Fermi liquid electronic excitations.

These ϵ-expansion results for the Bose–Fermi Kondo model were initially used to study the full self-consistent problem [15] with the self-consistency conditions specified in the previous section. The fact that the critical exponent for the local susceptibility is equal to $1 - \epsilon$ (equation (11)) turns out to be essential for the existence of a local QCP solution. The self-consistent solution in the case of two-dimensional magnetic fluctuations has $\epsilon = 1^-$, corresponding (equation (11)) to a logarithmically divergent local susceptibility.

3.3. Fractional exponent

The EDMFT equations in the Ising case (taking only the $a = z$ component) were studied numerically in [20, 21], using the quantum Monte Carlo method of Grempel and Rozenberg [31, 32].

It was found that, at the magnetic QCP, the local spin susceptibility is indeed logarithmically divergent. Figure 1 shows a log–log plot of the local spin susceptibility $\chi_{\mathrm{loc}}(\tau)$ versus $\sin(\pi\tau/\beta)$ at a relatively low temperature ($T = 0.011 T_K^0$). It is seen from the figure that the zero-temperature limit of the local susceptibility is $\chi_{\mathrm{loc}}(\tau) = A/\tau$. This corresponds to a frequency dependence that is logarithmically divergent in the low frequency limit. A fit of the data yields the value of the amplitude A that is directly related to the critical exponent of the peak value of the lattice susceptibility.

Figure 2 shows the logarithmic dependence of $\chi_{\mathrm{loc}}(\omega_n)$ directly, for frequencies smaller than the bare Kondo scale T_K^0. As already mentioned in the previous subsection, such a divergent local susceptibility signifies that the Bose–Fermi Kondo model is located on the
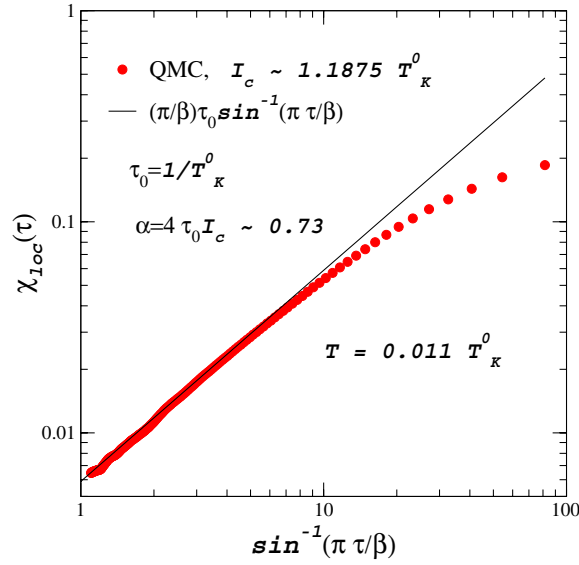
Figure 1. The local spin susceptibility χ_{loc} at the quantum critical coupling ($I \approx I_c$) as a function of the imaginary time τ. The log of χ_{loc} is plotted against the log of $\sin^{-1}(\pi\tau/\beta)$. The long-time limit, $\tau \to \beta/2$, corresponds to $\sin^{-1}(\pi\tau/\beta) \to 1$. The solid line is a fit in terms of $(\pi/\beta)\tau_0 \sin^{-1}(\pi\tau/\beta)$. The fit yields a dynamical spin susceptibility exponent $\alpha \approx 0.73$.
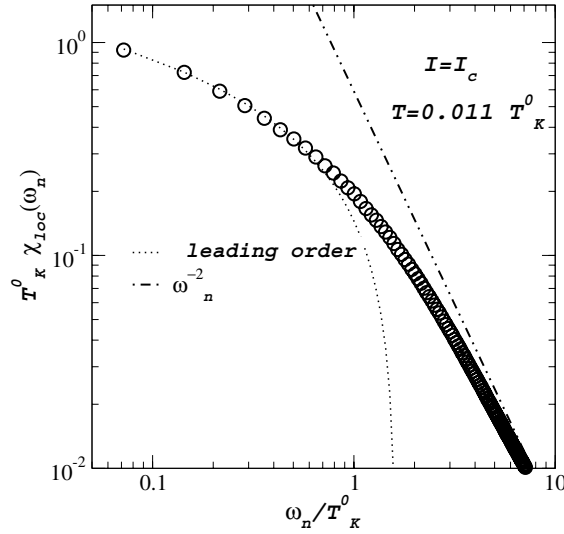

Figure 2. Plot (log–log) of the local spin susceptibility, χ_{loc} versus the Matsubara frequency, ω_n, at both low frequencies and high frequencies. The dotted curve marked 'leading order' corresponds to a logarithmic dependence of χ_{loc} on the frequency. The dot–dashed curve describes the fitting at high frequencies (not shown); the ω_n^{-2} dependence is dictated by the spectral sum rule.

critical manifold; correspondingly, there is a destruction of Kondo screening at the magnetic QCP of the Kondo lattice model.

From the divergent local susceptibility, the self-consistency equation (9) also determines the spin self-energy and, by extension, the dynamical spin susceptibility of the Kondo lattice.
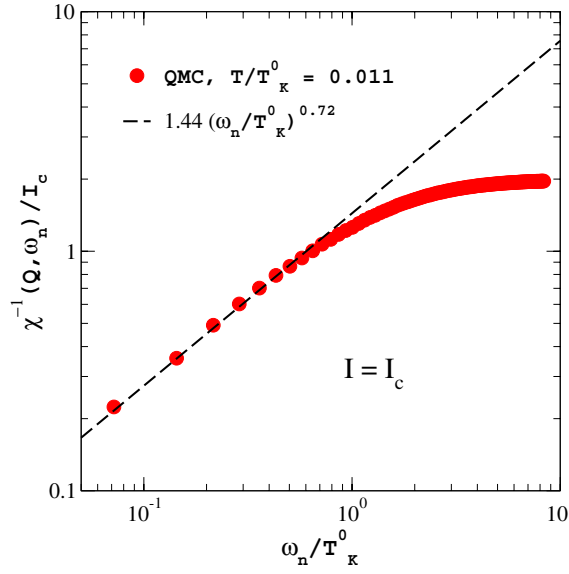
Figure 3. Inverse peak susceptibility versus. Matsubara frequency, at a low temperature ($T = 0.011 T_K^0$). We have used the asymptotic form appearing in the second equality of equation (9). The dashed line is a power-law fitting with the exponent 0.72.

The inverse peak susceptibility, $\chi^{-1}(\mathbf{Q}, \omega_n)$, where $\mathbf{Q}$ is the ordering wavevector, is shown in figure 3. A power-law fit yields a dynamical spin susceptibility exponent that is fractional, close to 0.72.

The fractional critical exponent is only seen at $|\omega_n| < T_K^0$. Likewise, the Fermi liquid (linear in ω_n) damping inside the paramagnetic phase is also seen only at frequencies up to at most T_K^0.

It is instructive to compare the above results with those of [22], which studied an Anderson lattice model. The lowest temperature studied in [22] is $0.25 T_K^0$. The first non-zero Matsubara frequency, $\omega_1 = 2\pi T$, is already larger than T_K^0. As a result, neither the fractional exponent at the critical coupling $I \sim I_c$ nor the linear damping at $I < I_c$ can be observed.

3.4. Failure of the local ϕ^4 description of the Bose–Fermi Kondo model

It is tempting to consider the Bose–Fermi Kondo model as equivalent to a local ϕ^4 theory. One maps the Kondo coupling to an Ising chain (along the imaginary time τ axis) with $1/\tau^2$ interactions [33]. In addition, the bosonic bath, with a spectrum of equation (10), adds an additional retarded interaction, $1/\tau^{2-\epsilon}$. The corresponding local ϕ^4 theory is $Z \sim \int \mathcal{D}\phi \exp[-S]$ where

$$S = \sum_{\omega_n} \left(r + \frac{1}{g_c}|\omega_n|^2 + \kappa_b|\omega_n|^{1-\epsilon} + \kappa_c|\omega_n| \right)|\phi(\omega_n)|^2 \qquad (12)$$

with the constraint $|\phi|^2 = 1$. Indeed, such a local ϕ^4 theory emerges in the large N limit of a certain O(N) generalization of the Bose–Fermi Kondo model. In the $N = \infty$ case, two of us [20] showed that, while the destruction of Kondo screening does occur, the fractional exponent is absent. Subsequently, Pankov *et al* [24] demonstrated that this conclusion remains valid to order $1/N$.

Recent works have considerably clarified the limitations of the large N limit and demonstrated the failure of the local ϕ^4 description of the Bose–Fermi Kondo model, at least for $\epsilon \geqslant 1/2$ (including the case of self-consistent $\epsilon = 1^-$). For the local ϕ^4 theory, $\epsilon = 1/2$ is the 'upper critical dimension' [34]. At $\epsilon > 1/2$, the critical point would then be Gaussian, implying violations of both ω/T scaling and hyperscaling. A number of recent studies on the Bose–Fermi Kondo and closely related impurity models [35–38], have shown that the quantum critical point is interacting over the entire range $0 < \epsilon < 1$, obeying ω/T scaling and hyperscaling. These results support the observation [20] of ω/T scaling in the (self-consistent) case of $\epsilon = 1^-$. They also imply that the Bose–Fermi Kondo model is perhaps the simplest model in which the standard description of a QCP—in terms of a classical critical point in elevated dimensions—fails. Physically, the Kondo effect, involving the formation of a Kondo singlet, is intrinsically quantum mechanical. In the language of a path integral representation for spin, the Kondo singlet formation necessarily involves the Berry phase term. It is then natural for the destruction of Kondo screening to be inherently quantum mechanical and, by extension, for the QCP of the Bose–Fermi Kondo model to be different from its classical counterpart at a higher dimension. A more in-depth understanding of the underlying mechanism for this effect will surely be illuminating.

4. Magnetic phase diagram of Kondo lattices within EDMFT

We now address whether the above results, derived from the paramagnetic side, are pre-empted by magnetic ordering. To do so, we approach the transition from the ordered side.

4.1. The EDMFT approach from the ordered side

The EDMFT equations for the antiferromagnetically ordered phase require normal ordering [16–18] of H_{f}: $H_{\mathrm{f}} = \sum_{ij} I_{ij}(\frac{1}{2} : S_i^z :: S_j^z : + \langle S_j^z \rangle S_i - \frac{1}{2} \langle S_i^z \rangle \langle S_j^z \rangle)$, where the normal-ordered operator is $: S_i^z :\equiv S_i^z - \langle S_i^z \rangle$. The effective impurity model and the self-consistency conditions are similar to equations (7) and (8), except for the following modifications. First, there is a local magnetic field—the static Weiss field, h_{loc}—coupled to S^z. This local field, arising through $I_{\mathbf{Q}}$, must be self-consistently determined by the magnetic order parameter $\langle S^z \rangle_{\mathrm{H_{imp}}}$.

Second, the conduction electron propagators are also influenced by magnetism. It turns out that the second feature has to be treated with care so that there is no double counting of the RKKY interactions between the local moments. In [21], we avoided double counting the RKKY interactions by working with a featureless conduction electron band; in this case, the magnetism is driven by the interaction $I_{\mathbf{q}}$ already incorporated at the Hamiltonian level (in H_{f}). We will expand on this issue in the next section.

Our phase diagram is shown in figure 4. At $I < I_{\mathrm{c}}$, the system is in the paramagnetic metal phase. The coherence scale of the Kondo lattice $E_{\mathrm{loc}}^\star$ marks the temperature/energy below which Kondo resonances are generated and the heavy Fermi liquid behaviour occurs. In particular, the Landau damping is linear in frequency at $|\omega_n| < E_{\mathrm{loc}}^\star$. At $I > I_{\mathrm{c}}$, the system has an antiferromagnetic ground state. There is a finite temperature first-order transition at the Néel temperature, T_{N}. However, T_{N} continuously goes to zero as the RKKY interaction is reduced. Within the numerical accuracy, it vanishes as $I \to I_{\mathrm{c}}^+$ [21], the same place where $E_{\mathrm{loc}}^\star$ does so as $I \to I_{\mathrm{c}}^-$. Plotted in figure 4 is the magnetic order parameter, m_{AF}, at the lowest temperature studied, $T = 0.011 T_{\mathrm{K}}^0$. Again, it is seen to continuously go to zero as $I \to I_{\mathrm{c}}^+$.

Further support for the second-order nature comes from the study of a nominally paramagnetic solution at $I > I_{\mathrm{c}}$. This solution to the paramagnetic EDMFT equations
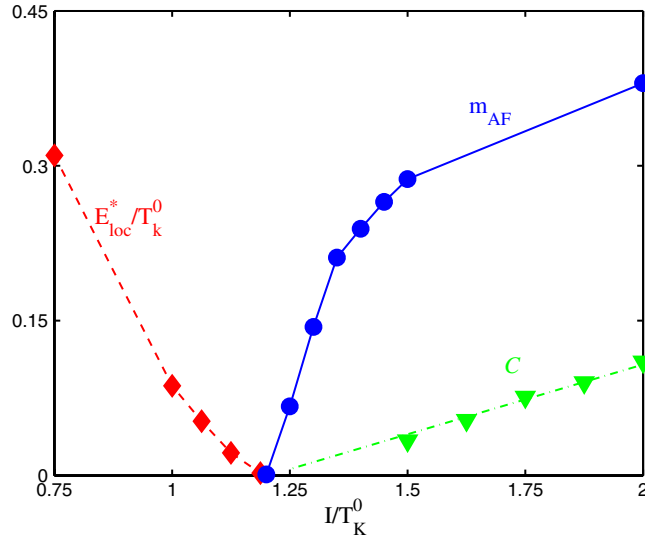
Figure 4. The coherence scale of the paramagnetic heavy fermion phase and the magnetic order parameter, m_{AF}, versus the tuning parameter, $\delta \equiv I/T_K^0$. Both quantities are determined at $T = 0.011T_K^0$. Also shown is the Curie constant of an unphysical solution without a magnetic order parameter at $\delta > \delta_c$. Lines are guides to the eye. The fact that all three curves meet at δ_c implies that the zero-temperature transition is continuous.

coexists with the solution to the ordered EDMFT equations at $I > I_c$. But this 'paramagnetic' solution is found to contain a Curie component C/T in the static local susceptibility with $C = \lim_{T \to 0} T \chi_{loc}(T, \omega_n = 0)$ or, equivalently, a jump of magnitude C/T in $\chi_{loc}(T, \omega_n)$ as ω_n goes to zero. (Its spin self-energy at zero frequency and zero temperature tracks I.) What this implies is that the 'paramagnetic' solution is not the physical one; instead, the physical ground state corresponds to the magnetic solution. Nonetheless, the study of this unphysical paramagnetic solution is helpful to the determination of the zero-temperature transition. It is seen in figure 4 that C extrapolates to zero at the same value of I_c ($I \to I_c^+$) at which $E_{loc}^\star$ goes to zero ($I \to I_c^-$). This provides an additional consistency check for the critical interaction where the paramagnetic phase terminates.

To summarize figure 4, within numerical accuracy, all relevant scales vanish simultaneously at I_c, and the quantum transition at zero temperature is continuous.

4.2. Avoiding double counting of the RKKY interaction

To discuss the double-counting issue in some detail, we revisit the procedure by which antiferromagnetism is treated in the standard DMFT [28]. Here, the dynamical equations are constructed entirely in terms of local single-particle quantities; two-particle responses are derived once the dynamical equations have been solved. On the paramagnetic side, the two-particle susceptibility satisfies the following Bethe–Salpeter equation (in matrix form):

$$\chi^{-1}(\mathbf{q}, \omega) = \chi_{p-h}^{-1}(\mathbf{q}, \omega) - I_{ir}(\mathbf{q}, \omega). \tag{13}$$

Here $\chi_{p-h}(\mathbf{q}, \omega)$ is the particle–hole susceptibility bubble of the full single-particle propagators $G(\mathbf{k}, \epsilon)$. The triplet particle–hole irreducible vertex has the following form (again, in matrix form) [39, 40]:

$$I_{ir}(\mathbf{q}, \omega) = \chi_{p-h,loc}^{-1}(\omega) - \chi_{loc}^{-1}(\omega), \tag{14}$$

where $\chi_{\mathrm{p-h,loc}}(\omega)$ is the particle–hole susceptibility bubble of the full local single-particle propagators $G_{\mathrm{loc}}(\epsilon)$. Combining this with equation (13) implies that, on the paramagnetic side,

$$\chi^{-1}(\mathbf{q}, \omega) = \Delta I_{\mathbf{q}} + \chi_{\mathrm{loc}}^{-1}(\omega) \tag{15}$$

where

$$\Delta I_{\mathbf{q}} \equiv \chi_{\mathrm{p-h}}^{-1}(\mathbf{q}, \omega) - \chi_{\mathrm{p-h,loc}}^{-1}(\omega). \tag{16}$$

For our Kondo lattice model, $\Delta I_{\mathbf{q}}$ has the meaning of the generated RKKY interaction (after inverting the matrix in the (f, c) space). How can $\Delta I_{\mathbf{q}}$ appear in the (particle–hole) spin response and not contribute in the dynamical equations for the single-particle quantities? The answer lies in the way in which the Brillouin zone is divided in DMFT into 'special' $\mathbf{q}$s and 'generic' $\mathbf{q}$s [41]. $\Delta I_{\mathbf{q}}$ of equation (16) is non-zero only at 'special' $\mathbf{q}$s. The dynamical equations are constructed in terms of quantities that are local, i.e. summed over $\mathbf{q}$: the special $\mathbf{q}$s, having measure zero, are not important for this summation; only 'generic' $\mathbf{q}$s have the phase space to contribute to the local quantities. To be more specific, consider the hypercubic lattice. $\Delta I_{\mathbf{q}}$ depends on $\mathbf{q}$ only through the combination $X(\mathbf{q}) = (1/d) \sum_{\alpha=1}^{d} \cos(q_\alpha)$ [41]. The dispersion $X(\mathbf{q})$ is O(1) (in the $d \to \infty$ limit) only for 'special' $\mathbf{q}$s, e.g. along the diagonals of the Brillouin zone, $q_1 = q_2 = \cdots = q_d$. On the other hand, for 'generic' $\mathbf{q}$, $X(\mathbf{q})$ vanishes (being formally of order $O(1/\sqrt{d})$, as can be seen from the central limit theorem). When $X(\mathbf{q})$ vanishes, $\chi_{\mathrm{p-h}}(\mathbf{q}, \omega) = \chi_{\mathrm{p-h,loc}}(\omega)$, so $\Delta I_{\mathbf{q}}$ vanishes! The antiferromagnetic wavevector $\mathbf{Q}$ ($Q_\alpha = \pi$ for all α), belongs to the set of special $\mathbf{q}$s, so $\Delta I_{\mathbf{Q}} \neq 0$. And the antiferromagnetic instability, from the paramagnetic side, is signalled by $\chi^{-1}(\mathbf{Q}, \omega) = \Delta I_{\mathbf{Q}} + \chi_{\mathrm{loc}}^{-1}(\omega) = 0$, at $\omega = 0$. On the antiferromagnetic side, the non-zero value for the corresponding $\Delta I_{\mathbf{Q},\mathrm{or}}$ is implemented through the introduction of the doubling of the conduction electron unit cell and different single-particle propagators at the two sublattices. Formally, this doubling of the conduction electron unit cell can be described in terms of an effective susceptibility, $\chi_{\mathrm{or}}(\mathbf{Q}, \omega)$:

$$\chi_{\mathrm{or}}^{-1}(\mathbf{Q}, \omega) = \Delta I_{\mathbf{Q},\mathrm{or}} + \chi_{\mathrm{loc}}^{-1}(\omega). \tag{17}$$

Here, again, $\Delta I_{\mathbf{Q},\mathrm{or}} = \chi_{\mathrm{p-h}}^{-1}(\mathbf{Q}, \omega) - \chi_{\mathrm{p-h,loc}}^{-1}(\omega)$. The instability of the ordered state is signalled by $\chi_{\mathrm{or}}^{-1}(\mathbf{Q}, \omega) = \Delta I_{\mathbf{Q},\mathrm{or}} + \chi_{\mathrm{loc}}^{-1}(\omega) = 0$, also at $\omega = 0$. Because the effective RKKY interaction incorporated on the ordered side, $\Delta I_{\mathbf{Q},\mathrm{or}}$, is the same as its counterpart on the paramagnetic side, $\Delta I_{\mathbf{Q}}$, the magnetic transition is in general of second order. There is a major limitation to this approach. The RKKY interaction, being zero at generic wavevectors, does not have enough phase space to dynamically interplay with the Kondo interaction. So the self-consistent dynamical equations of DMFT do not incorporate $\Delta I_{\mathbf{q}}$ at all, and the Kondo screening is always present including at the magnetic QCP. The quantum critical behaviour falls in the SDW category, as in any static mean field description of Kondo lattices.

The EDMFT is introduced precisely to allow this dynamical interplay. Here, an intersite interaction, as given in H_f of equation (2), is elevated to the Hamiltonian level. The Bethe–Salpeter equation (13) still applies. However, the particle–hole irreducible vertex becomes [17]

$$I_{\mathrm{ir}}(\mathbf{q}, \omega) = \chi_{\mathrm{p-h,loc}}^{-1}(\omega) - \chi_{\mathrm{loc}}^{-1}(\omega) - \chi_0^{-1}(\omega) - I_{\mathbf{q}}, \tag{18}$$

where $I_{\mathbf{q}}$ is the Fourier transform of the intersite interactions, I_{ij}, already included at the Hamiltonian level. We have, on the paramagnetic side,

$$\chi^{-1}(\mathbf{q}, \omega) = \Delta I_{\mathbf{q}} + I_{\mathbf{q}} + M(\omega), \tag{19}$$

where $M(\omega) = \chi_{\text{loc}}^{-1}(\omega) + \chi_0^{-1}(\omega)$ is the spin self-energy. Likewise, we can write the effective susceptibility that comes into the stability analysis of the ordered phase as

$$\chi_{\text{or}}^{-1}(\mathbf{q}, \omega) = \Delta I_{\mathbf{q},\text{or}} + I_{\mathbf{q}} + M(\omega). \tag{20}$$

It was shown in [17] that the EDMFT can be rigorously formulated only when all $\mathbf{q}$ are considered to be generic. (Otherwise, $I_{\mathbf{q}}$ is formally of order $\text{O}(d)$ at the special $\mathbf{q}$s, and no paramagnetic phase could exist.) This implies that $\Delta I_{\mathbf{q}} = 0$ for all $\mathbf{q}$. From the Kondo lattice point of view, this is equivalent to saying that we will only use $I_{\mathbf{q}}$ to represent the RKKY interaction and will not incorporate additional RKKY interactions generated from the fermion bubbles (illustrated in figure 7 of [17]).

In order to be consistent, one would also need to demand that $\Delta I_{\mathbf{q},\text{or}} = 0$ on the ordered side. Otherwise, we would be counting *additional* contributions to the RKKY interaction on the ordered side that were absent on the paramagnetic side. This requirement ($\Delta I_{\mathbf{q},\text{or}} = 0$) was achieved in [21] by using a featureless conduction electron band. The latter ensures that all wavevectors are generic in the sense defined earlier. Within this procedure, the magnetic ordering is entirely driven by $I_{\mathbf{q}}$, and the instability criteria from the paramagnetic and ordered sides coincide. Therefore, the quantum transition is naturally of second order, as was indeed seen numerically in [21]; see figure 4 above.

The procedure used in [22] and [23] amounts, in our language, to keeping $\Delta I_{\mathbf{Q}} = 0$ while $\Delta I_{\mathbf{Q},\text{or}} \neq 0$. On the paramagnetic side, all wavevectors, including the ordering wavevector $\mathbf{Q}$, are taken as generic, and $\Delta I_{\mathbf{Q}} = 0$, as in all EDMFT schemes. On the ordered side, $\mathbf{Q}$ is considered as one of the special wavevectors in the sense defined earlier and, through the conduction electron unit-cell doubling, $\Delta I_{\mathbf{Q},\text{or}} \neq 0$ (as in DMFT). The ordered side then has an added energy gain, and the magnetic quantum transition is of first order. (That an EDMFT approach to Kondo lattices which incorporate a DMFT-like fermion bubble on the ordered side alone yields a first-order transition at zero temperature was in fact already recognized in [23].) The procedure would actually lead to a first-order magnetic transition at zero temperature in any itinerant model, including any $T = 0$ SDW transition without any Kondo physics.

We close by noting that the different EDMFT schemes that we have discussed can be equivalently seen as different local approximations to a Baym–Kadanoff-type functional.

5. Experiments and other theoretical approaches

An important manifestation of the destruction of the Kondo screening is that f electrons participate in the Fermi volume on the paramagnetic side but fail to do so on the antiferromagnetic side. There is a sudden reconstruction of the Fermi surface across the magnetic QCP. Fairly direct electronic evidence of this effect has appeared in the recent Hall effect measurement for YbRh$_2$Si$_2$ [42]. The Hall coefficient shows a rapid crossover as a function of the control parameter—the magnetic field in this case. The crossover sharpens as temperature is lowered, extrapolating to a jump in the zero-temperature limit. The jump occurs at the extrapolated location of the magnetic phase boundary at zero temperature. Related features have also been observed for YbAgGe [43].

A more direct probe of the Fermi surface comes from the de Haas–van Alphen effect. Recent dHvA measurements [44] for CeRhIn$_5$ provide tantalizing evidence of a large reconstruction of the Fermi surface, with a divergent effective mass, at a QCP. Specific heat measurement under a magnetic field [45] points to the possibility that CeRhIn$_5$ undergoes a second-order magnetic quantum transition at the magnetic field of the strength used in the dHvA experiment. If the existence of the magnetic QCP is indeed established, CeRhIn$_5$ will provide more insights into quantum criticality than CeRh$_2$Si$_2$. In the latter system, a large Fermi surface reconstruction has also been seen in the dHvA measurements [46], but the

zero-temperature transition is likely to be first order with a large jump in the magnetic order parameter across the transition.

The fractional exponent and ω/T scaling in the magnetic dynamics have been seen, since early on, in the antiferromagnetic QCP of Au-doped CeCu$_6$ [11, 12] (whose magnetic fluctuations have a reduced dimensionality) and in some frustrated compounds [13, 14]. (On the other hand, the SDW behaviour is observed in the magnetic dynamics of Ce(Ru$_{1-x}$Rh$_x$)$_2$Si$_2$ [47], which has quasi-3D magnetic fluctuations.) Related non-trivial scaling exponents—that are relatively easy to connect with theory–have come from the Grüneisen ratio [48].

Theoretically, there have also been efforts to study the Kondo lattice systems using certain mixed boson–fermion representations for the local moment spin operators [49–51]. Such auxiliary-particle representations set up the basis for a picture with spin–charge separation. However, it has been hard to use this formalism to properly capture the Kondo screened Fermi liquid phase [52], making it difficult to study its destruction as well.

It may also be possible to describe the destruction of Kondo screening in terms of the static mean field theories based on the slave boson and an RVB order parameter, supplemented by gauge field fluctuations. The corresponding phase diagram has recently been studied in some detail [53]. The magnetic transition and destruction of the Kondo screening are found to occur at different places in the zero-temperature phase diagram [53], so the magnetic quantum transition is still of the SDW type. We believe that this is a reflection of the static nature of the mean field theory.

Finally, it is instructive to put in the present context the QCP proposed for the transition from an antiferromagnet to a valence bond solid in frustrated quantum magnets [54]. Dubbed a 'deconfined' QCP, it has certain properties that may be qualitatively compared with the local quantum criticality: the QCP—containing exotic excitations—is surrounded by two conventional phases, and the corresponding energy scales of both vanish as the QCP is approached. Hence, it would be enlightening to explore the concrete connections (if any) of this approach with the physics of the destruction of Kondo screening. For this purpose, it would be necessary to either construct microscopic spin models for the deconfined QCP or reformulate the Kondo screening beyond microscopic approaches.

6. Summary and outlook

To summarize, we have discussed some of the microscopic approaches underlying the local quantum critical picture. Beyond the initial studies based on an ϵ-expansion renormalization group method, the most extensive investigations have been carried out in Kondo lattice models with Ising anisotropy. The latter have allowed the study of both the destruction of Kondo screening and the concomitant fractional exponent and ω/T scaling in the magnetic dynamics. We have also discussed the magnetic phase diagram and summarized the evidence for the second-order nature of the magnetic quantum phase transition. The EDMFT studies of Kondo lattice models with continuous spin symmetry ($SU(2)$ or XY) are mostly confined to ϵ-expansion studies. Efforts to access the quantum critical point in these systems, beyond the ϵ-expansion, are still under way. A dynamical large N limit, for instance, has recently been shown to be promising [35].

The microscopic approaches described here have shown that critical modes beyond the order parameter fluctuations exist, and the modes are associated with the destruction of Kondo screening. These insights have a number of phenomenological consequences—not only in magnetic dynamics but also in the Fermi surface properties and in thermodynamics—which have been supported by existing and emerging experiments. The insights will also help in the search for a field theory that describes quantum critical heavy fermions. Finally, they may very

well be broadly relevant to the exotic quantum critical behaviour in other strongly correlated systems such as doped Mott insulators.

Acknowledgments

References

[1]   Stewart G R 1984 *Rev. Mod. Phys.* **56** 755
[2]   Doniach S 1977 *Physica* B **91** 231
[3]   Varma C M 1976 *Rev. Mod. Phys.* **48** 219
      Varma C M, Nussinov Z and van Saarloos W 2002 *Phys. Rep.* **361** 267
[4]   Bickers N E 1987 *Rev. Mod. Phys.* **59** 845
[5]   Stewart G R 2001 *Rev. Mod. Phys.* **73** 797
[6]   Sachdev S 2000 *Science* **288** 475
[7]   Hertz J A 1976 *Phys. Rev.* B **14** 1165
[8]   Millis A J 1993 *Phys. Rev.* B **48** 7183
[9]   Moriya T and Takimoto T 1995 *J. Phys. Soc. Japan* **64** 960
[10] Lonzarich G G 1997 *Electron* ed M Springford (Cambridge: Cambridge University Press) p 109
[11] Schröder A, Aeppli G, Coldea R, Adams M, Stockert O, von Löhneysen H, Bucher E, Ramazashvili R and Coleman P 2000 *Nature* **407** 351
[12] Stockert O, von Löhneysen H, Rosch A, Pyka N and Loewenhaupt M 1998 *Phys. Rev. Lett.* **80** 5627
[13] Aronson M C, Osborn R, Robinson R A, Lynn J W, Chau R, Seaman C L and Maple M B 1995 *Phys. Rev. Lett.* **75** 725
[14] Wilson S D, Dai P, Adroja D T, Lee S-H, Chung J-H, Lynn J W, Butch N P and Maple M B 2005 *Phys. Rev. Lett.* **94** 056402
[15] Si Q, Rabello S, Ingersent K and Smith J L 2001 *Nature* **413** 804
      Si Q, Smith J L and Ingersent K 1999 *Int. J. Mod. Phys.* B **13** 2331
[16] Si Q and Smith J L 1996 *Phys. Rev. Lett.* **77** 3391
[17] Smith J L and Si Q 2000 *Phys. Rev.* B **61** 5184
[18] Chitra R and Kotliar G 2000 *Phys. Rev. Lett.* **84** 3678
      Kajueter H 1996 *PhD Thesis* Rutgers University
[19] The EDMFT approach shares similarity to, but is more general than, the dynamical equations developed in the spin-glass context: Ye J, Sachdev S and Read N 1993 *Phys. Rev. Lett.* **70** 4011
      Sengupta A M and Georges A 1995 *Phys. Rev.* B **52** 10295
      Bray A J and Moore M A 1980 *J. Phys. C: Solid State Phys.* **13** L655
[20] Grempel D R and Si Q 2003 *Phys. Rev. Lett.* **91** 026401
[21] Zhu J-X, Grempel D R and Si Q 2003 *Phys. Rev. Lett.* **91** 156404
[22] Sun P and Kotliar G 2003 *Phys. Rev. Lett.* **91** 037209
[23] Sun P and Kotliar G 2005 *Preprint* cond-mat/0501175
[24] Pankov S, Florens S, Georges A, Kotliar G and Sachdev S 2004 *Phys. Rev.* B **69** 054426
[25] Lacroix C 1985 *Solid State Commun.* **54** 991
[26] Nozières Ph 1998 *Eur. Phys. J.* B **6** 447
[27] Schiller A and Ingersent K 1995 *Phys. Rev. Lett.* **75** 113
[28] Georges A, Kotliar G, Krauth W and Rozenberg M J 1996 *Rev. Mod. Phys.* **68** 13
[29] Metzner W and Vollhardt D 1980 *Phys. Rev. Lett.* **62** 324
[30] Zhu L and Si Q 2002 *Phys. Rev.* B **66** 024426
      Zaránd G and Demler E 2002 *Phys. Rev.* B **66** 024427 and references therein

[31] Grempel D R and Rozenberg M J 1999 *Phys. Rev.* B **60** 4702
[32] Grempel D R and Rozenberg M J 1998 *Phys. Rev. Lett.* **80** 389
     Rozenberg M J and Grempel D R 1998 *Phys. Rev. Lett.* **81** 2550
[33] Anderson P W and Yuval G 1971 *J. Phys. C: Solid State Phys.* **4** 607
[34] Fisher M E, Ma S-K and Nickel B G 1976 *Phys. Rev. Lett.* **29** 917
     Kosterlitz J M 1976 *Phys. Rev. Lett.* **37** 1577
[35] Zhu L, Kirchner S, Si Q and Georges A 2004 *Phys. Rev. Lett.* **93** 267201
[36] Vojta M, Tong N and Bulla R 2005 *Phys. Rev. Lett.* **94** 070604
[37] Glossop M T and Ingersent K 2005 *Preprint* cond-mat/0501601
[38] Kirchner S, Park T-H, Si Q and Grempel D R 2005 unpublished
[39] Zlatic V and Horvatic B 1990 *Solid State Commun.* **75** 263
[40] Jarrell M 1995 *Phys. Rev.* B **51** 7429
[41] Müller-Hartmann E 1989 *Z. Phys.* B **74** 507
     Brandt U and Mielsch C 1989 *Z. Phys.* B **75** 365
[42] Paschen S, Lühmann T, Wirth S, Gegenwart P, Trovarelli O, Geibel C, Steglich F, Coleman P and Si Q 2004
     Nature **432** 881
[43] Bud'ko S L, Morosan E and Canfield P C 2005 *Phys. Rev.* B **71** 054408
[44] Shishido H, Settai R, Harima H and Ōnuki Y 2005 *J. Phys. Soc. Japan* **74** 1103
[45] Park T *et al* 2005 unpublished
     Thompson J D 2005 private communications
[46] Araki S, Settai R, Kobayashi T C, Harima H and Ōnuki Y 2001 *Phys. Rev.* B **64** 224417
[47] Kadowaki H, Tabata Y, Sato M, Aso N, Raymond S and Kawarazaki S 2005 *Preprint* cond-mat/0504386,
     unpublished
[48] Küchler R, Oeschler N, Gegenwart P, Cichorek T, Neumaier K, Tegus O, Geibel C, Mydosh J A, Steglich F,
     Zhu L and Si Q 2003 *Phys. Rev. Lett.* **91** 066405
[49] Coleman P and Pépin C 2003 *Acta Phys. Pol.* B **34** 691
[50] Pépin C 2005 *Phys. Rev. Lett.* **94** 066402
[51] Rech J and Coleman P 2005 unpublished
[52] Parcollet O and Georges A 1997 *Phys. Rev. Lett.* **79** 4665
[53] Senthil T, Vojta M and Sachdev S 2004 *Phys. Rev.* B **69** 035111
[54] Senthil T, Vishwanath A, Balents L, Sachdev S and Fisher M P A 2004 *Science* **303** 1490